Supporting Information

# Highly Reversible Aqueous Zinc Metal Batteries Enabled by Fluorinated Interphases in Localized High Concentration Electrolytes

Shunqiang Chen[a], Qingshun Nian[a], Lei Zheng[b], Bing-qing Xiong[a], Zihong Wang[a] Yanbin Shen[b,*], Xiaodi Ren[a,*]

S. Chen, Q. Nian, B. Xiong, Z. Wang, Prof. X. Ren*

[a] Hefei National Laboratory for Physical Science at the Microscale, CAS Key Laboratory of Materials for Energy Conversion, Department of Materials Science and Engineering, University of Science and Technology of China, Anhui 230026, China

Email: xdren@ustc.edu.cn

Lei Zheng, Prof. Y. Shen*

[b] i-Lab, CAS Center for Excellence in Nanoscience, Suzhou Institute of Nano-Tech and Nano-Bionics (SINANO), Chinese Academy of Sciences, Suzhou 215123, China

Email: ybshen2017@sinano.ac.cn

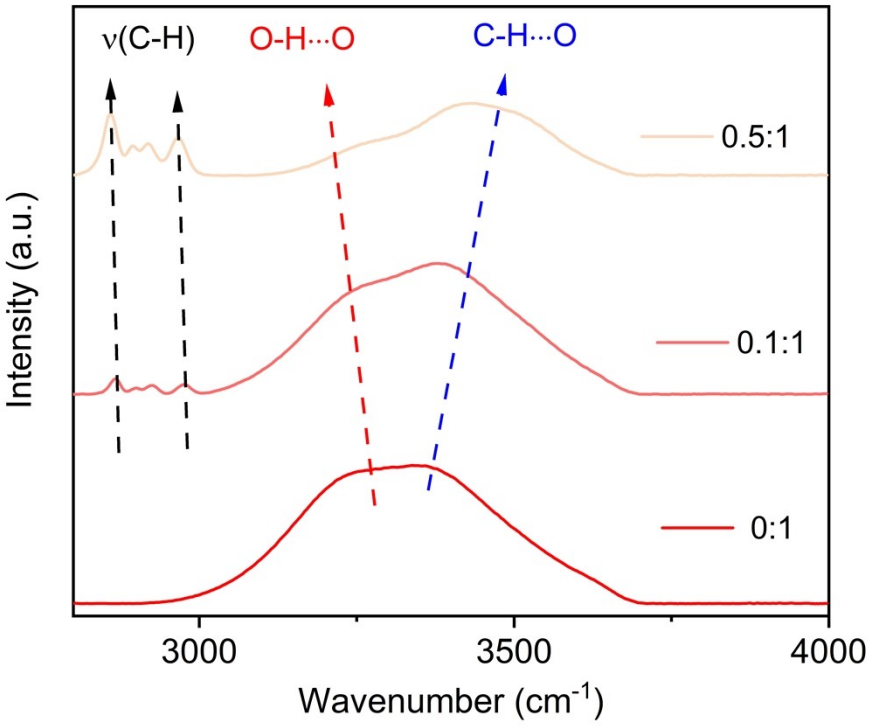


**Fig. S1.** The FTIR of $H_2O$ and 1,4-DX mixture solution with different molar ratios (1,4-DX: $H_2O$=x: 1).

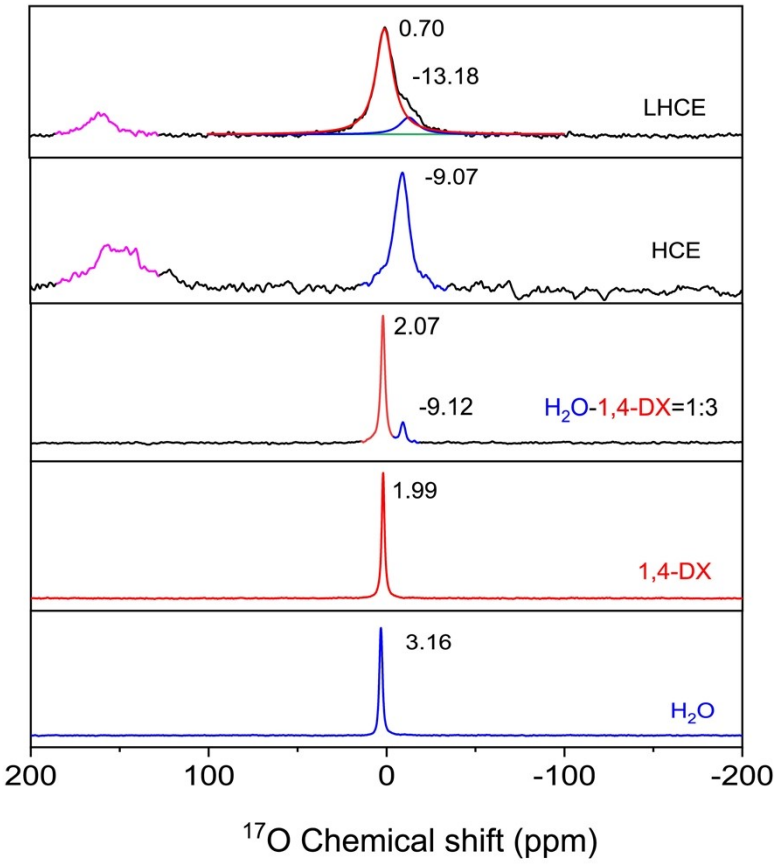


**Fig. S2.** $^{17}$O-NMR spectra of different solvents and electrolytes.

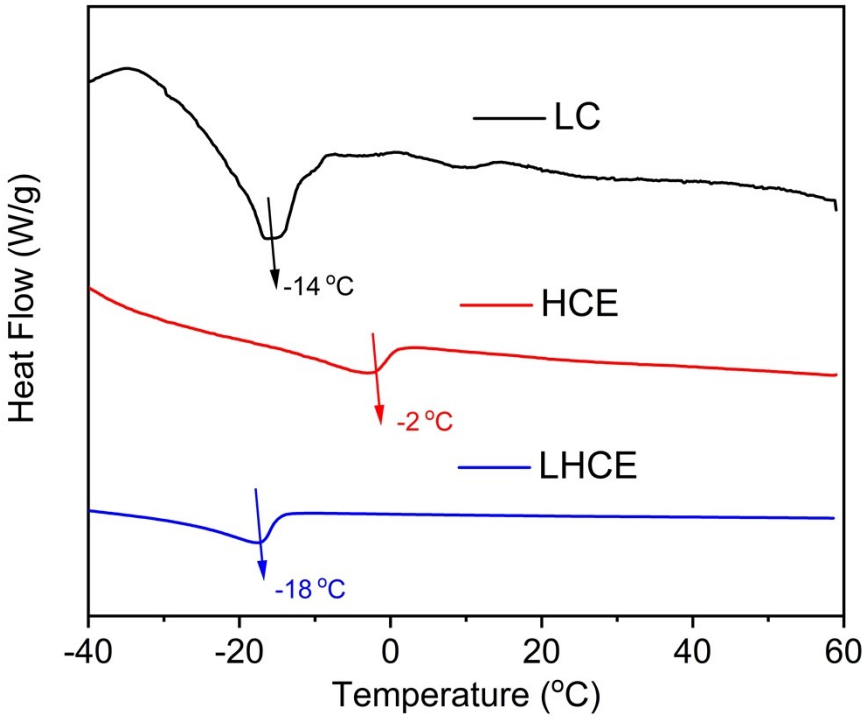


**Fig. S3.** DSC curves for LC, HCE and LHCE.

**Table S1.** Physical properties of different electrolytes

| **Sample** | **Conductivity (mS/cm)** | **Viscosity (**mPa•s**)** |
|---|---|---|
| $(TFSI)_{0.7}(BETI)_{0.3}$ | 2.2 | 562.3 |
| $(TFSI)_{0.7}(BETI)_{0.3}$-1-1 | 1.2 | 243.9 |
| $(TFSI)_{0.7}(BETI)_{0.3}$-1-2 | 3.1 | 45.5 |
| $(TFSI)_{0.7}(BETI)_{0.3}$-1-3 | 3.3 | 21.7 |

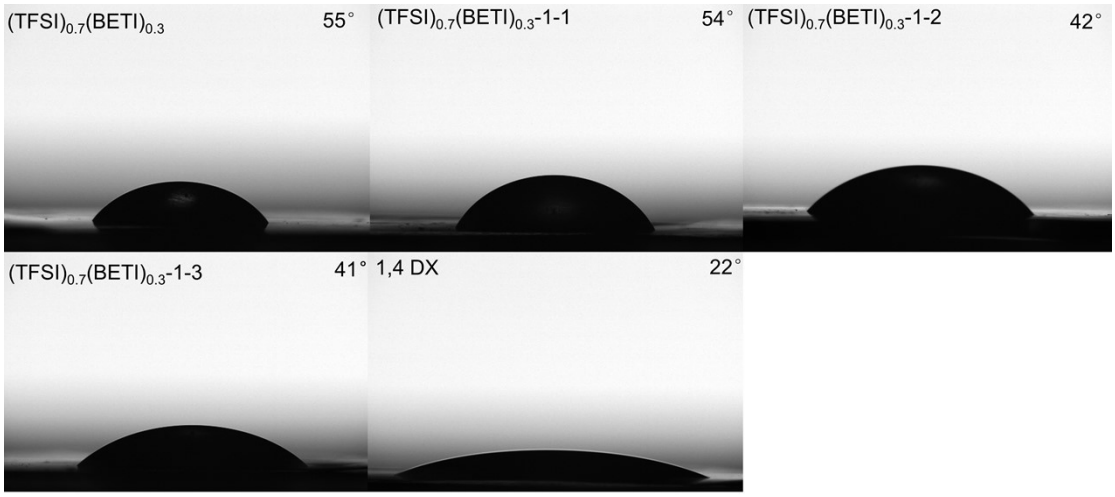


**Fig. S4.** Contact angles for different electrolytes on Zn foil.

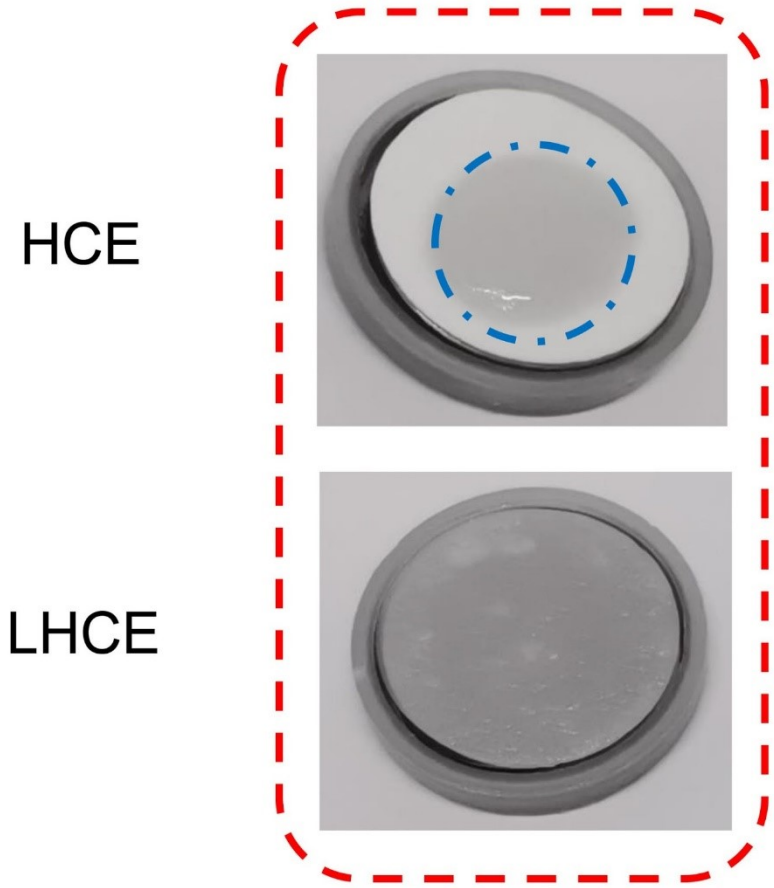


**Fig. S5.** Wettability tests of HCE and LHCE on separator using 75 µl electrolyte.

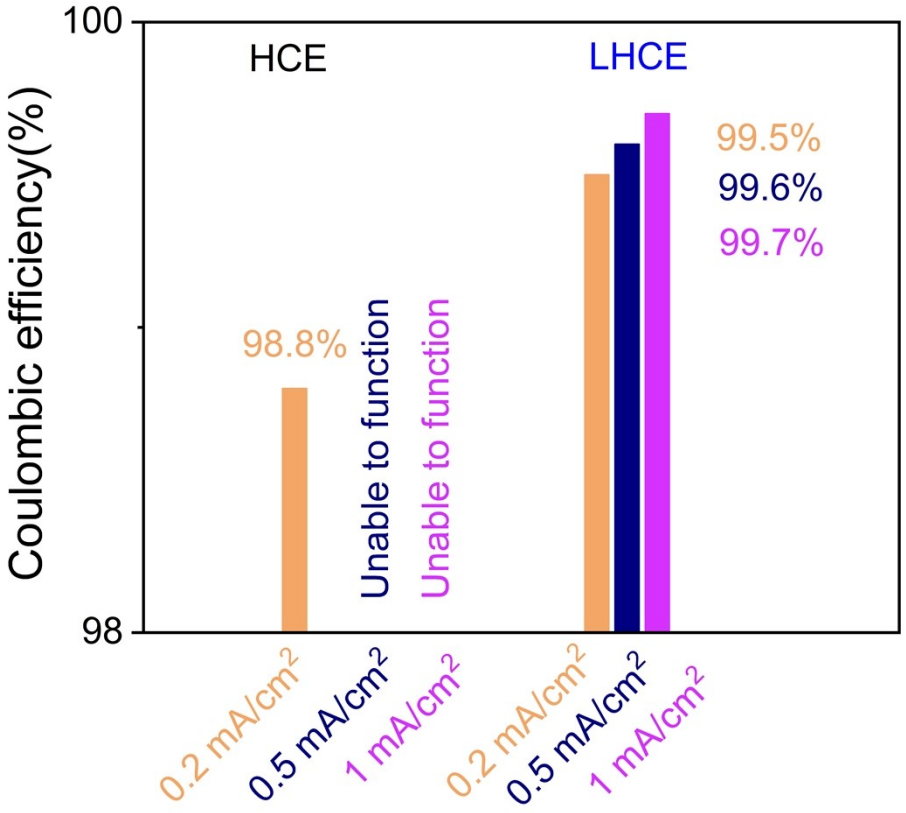


**Fig. S6.** The specific bar graph of Zn CE in the HCE and LHCE.

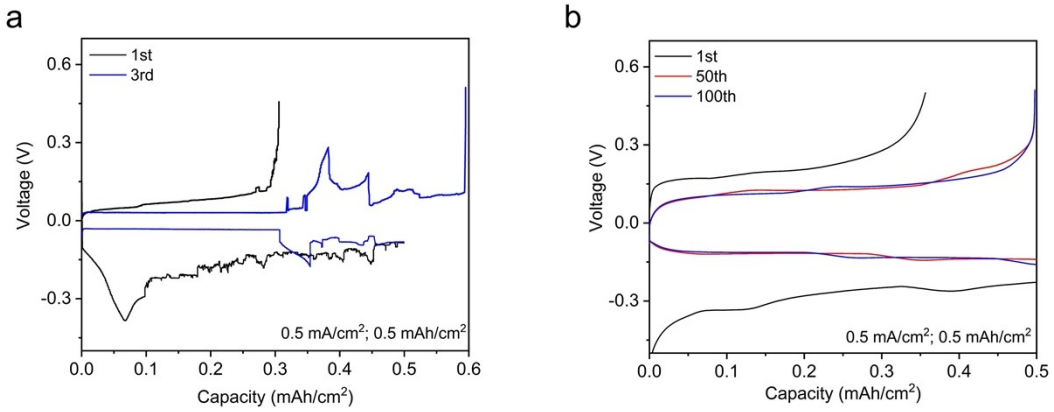


**Fig. S7.** Voltage profiles of Zn plating/stripping processes in (a) HCE and (b) LHCE at 0.5 mA/cm$^2$ and 0.5 mAh/cm$^2$.

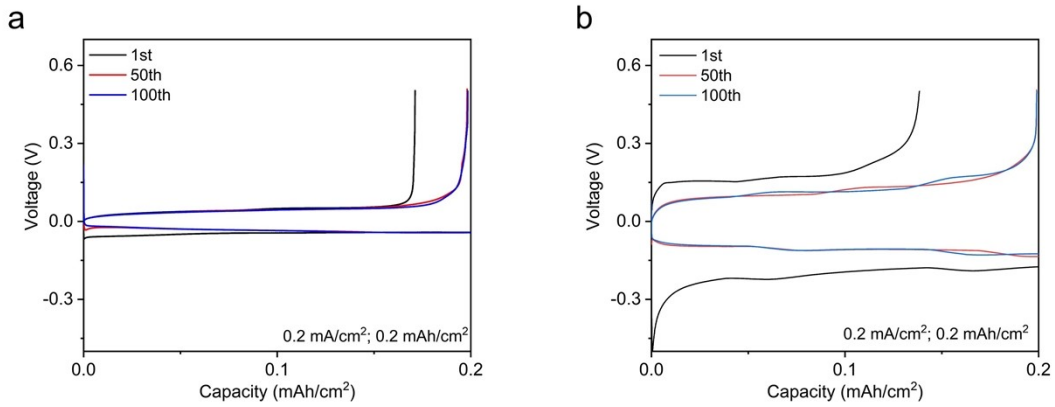


**Fig. S8.** Voltage profiles of Zn plating/stripping processes in (a) HCE and (b) LHCE at 0.2 mA/cm$^2$ and 0.2 mAh/cm$^2$.

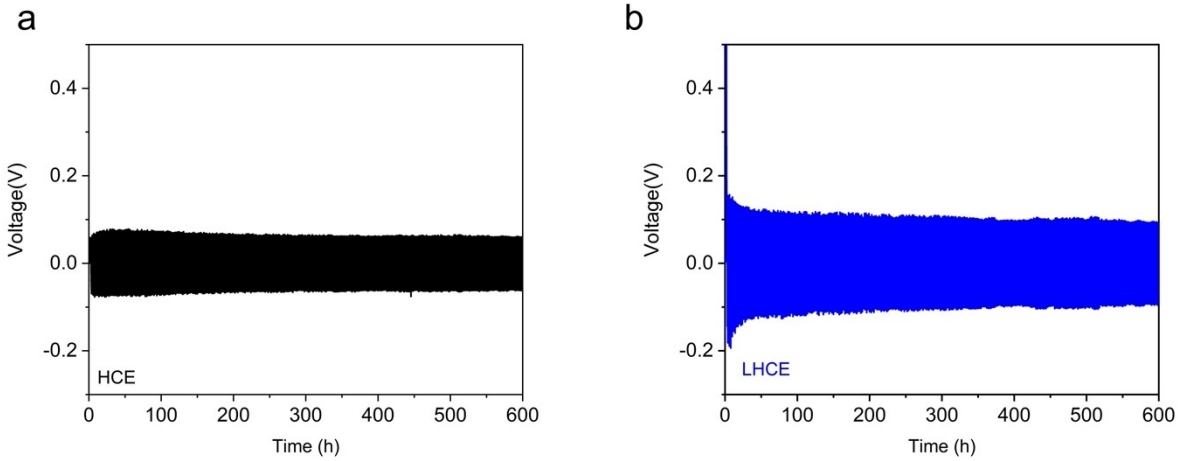


**Fig. S9.** Galvanostatic cyclings of Zn||Zn symmetrical cells at a current density of 0.2 mA/cm$^2$ and a capacity of 0.2 mAh/cm$^2$ in(a) HCE and (b) LHCE.

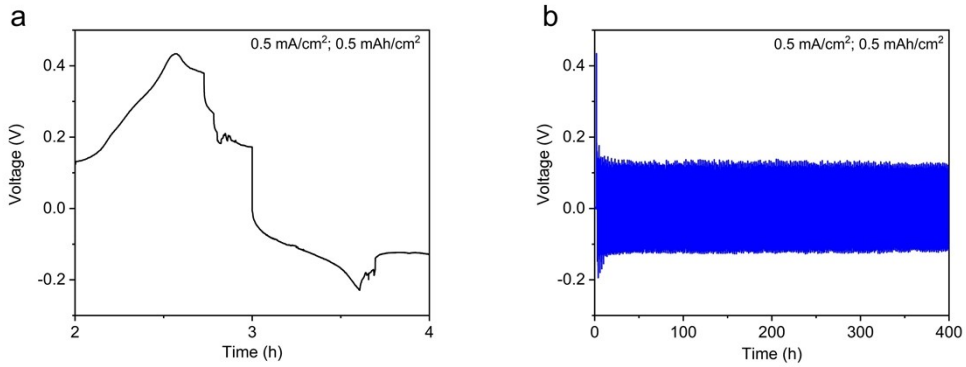


**Fig. S10.** Galvanostatic cyclings of Zn||Zn symmetrical cells at a current density of 0.5 mA/cm$^2$ and a capacity of 0.5 mAh/cm$^2$ in (a) HCE and (b) LHCE.

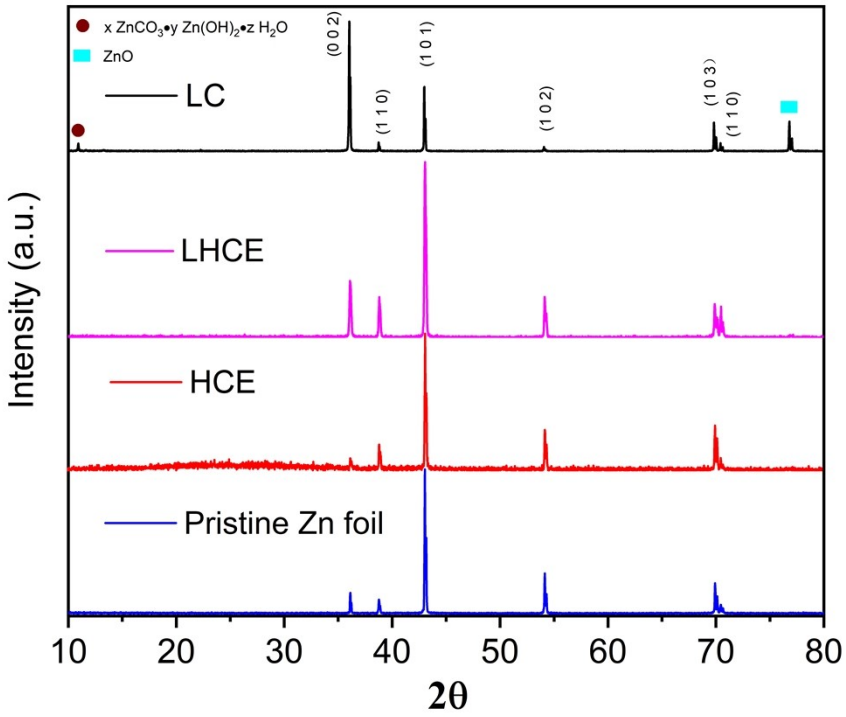


**Fig. S11.** XRD patterns of Zn anodes after Zn||Zn tests for 400 cycles in LHCE, HCE and 50 cycles in LC at 0.2 mA/cm$^2$ and 0.2 mAh/cm$^2$.

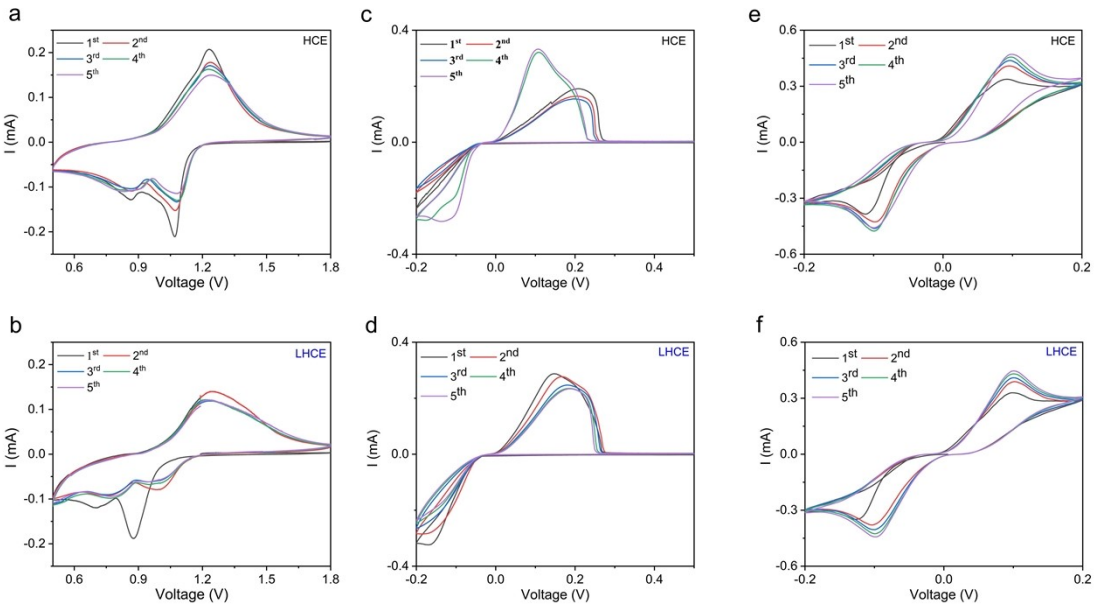


**Fig. S12.** CV of (a, b) Zn||$V_2O_5$, (c, d) Zn||Cu and (e, f) Zn||Zn cells in HCE and LHCEat 0.1 mV/s

Zn||Zn and Zn||Cu cells were assembled to investigate Zn compatibility with HCE and LHCE. The CV curve of Zn||Cu batteries show the better reversibility of Zn plating/stripping in LHCE (92%) compared to that in HCE (83%). Meanwhile, Zn||Zn cell shows the reversible redox reactions of Zn plating/stripping in both HCE and LHCE.

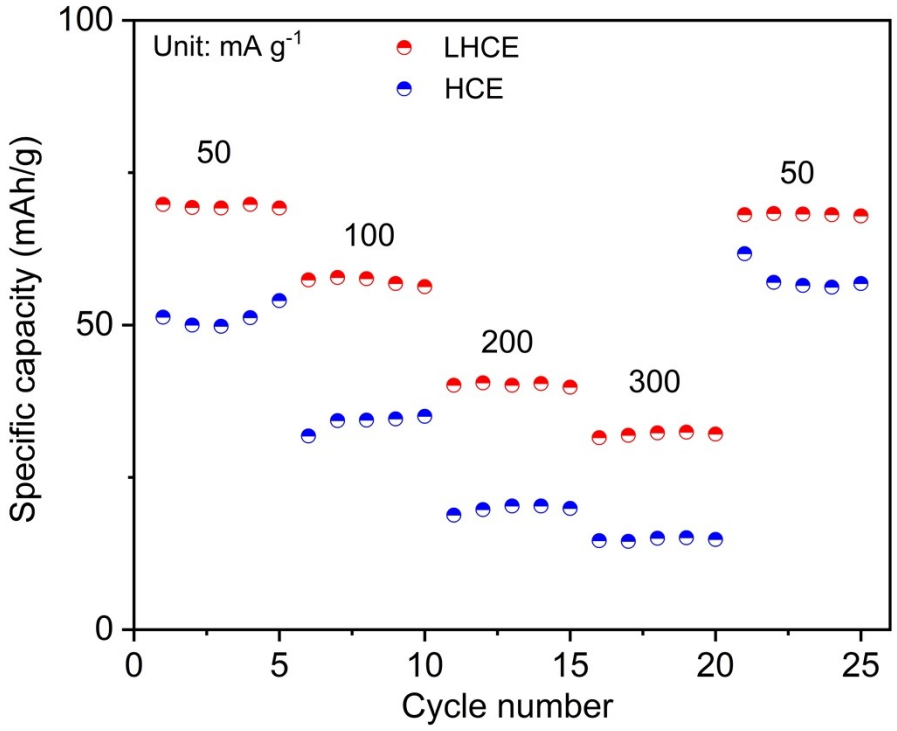


**Fig. S13.** Rate performances of Zn||$V_2O_5$ full cells in different electrolytes.

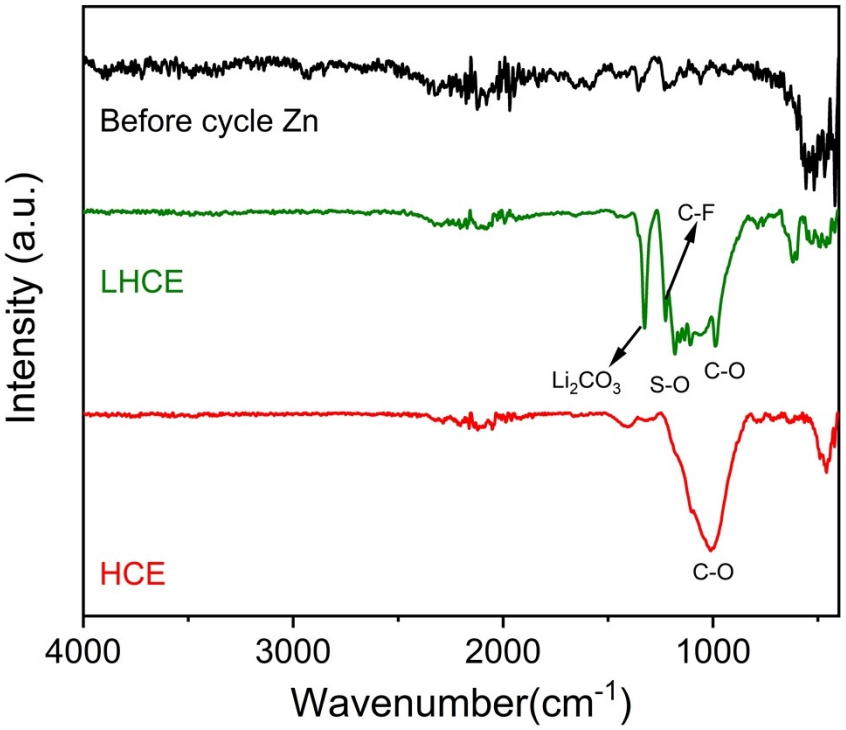


**Fig. S14.** FTIR spectra of Zn metal surface after 10 plating/stripping cycles in HCE and LHCE at a current density of 0.2 mA/cm$^2$.

The compositions of SEI layer in different electrolytes were characterized by FT-IR. More apparent signals from $Li_2CO_3$, C-F and S-O functional groups are observed on the Zn surface in LHCE compared to that in HCE, which are originated from the decomposition of $TFSI^-$ and $BETI^-$ anions. This further confirmed that the introduction of 1,4-DX into HCE promotes the decomposition of anions.

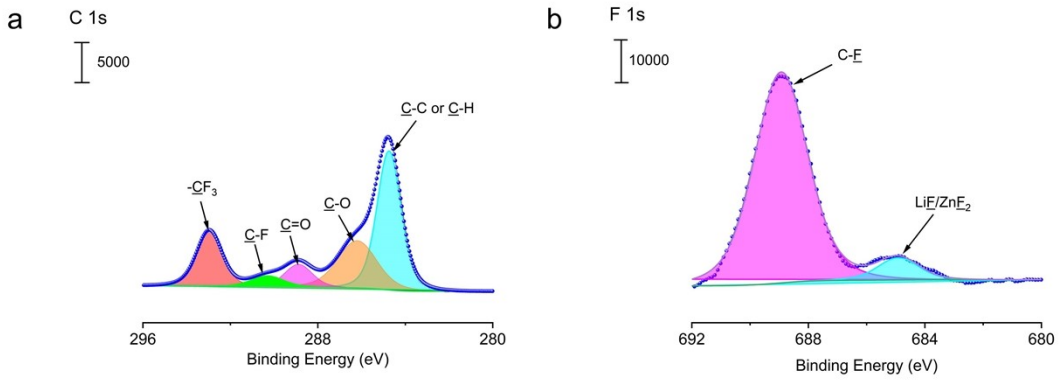


**Fig. S15.** XPS spectra of (a) C 1s and (b) F 1s for Zn metal after 10 plating/stripping cycles in HCE at a current density of 0.2 mA/cm$^2$.

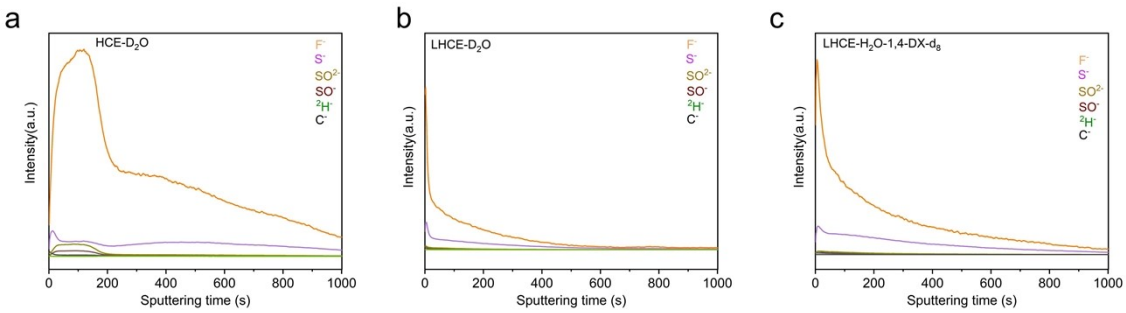


**Fig. S16.** TOF-SIMS analysis of the SEI on cycled Zn anodes in different electrolytes.

**Table S2. CE comparison of different aqueous electrolytes.**

| Electrolytes | Test protocol | Coulombic efficiency | Ref |
|---|---|---|---|
| LHCE | 1 $mA/cm^2$; 1 $mAh/cm^2$ | 99.7% | This Work |
| 1.6 m $ZnCl_2$-$H_2O$-dimethyl sulfoxide | 0.5 $mA/cm^2$; 1 $mAh/cm^2$ | 99.5% | [1] |
| 1 m $Zn(TFSI)_2$-acetamide | 0.5 $mA/cm^2$; 1 $mAh/cm^2$ | 99.7% | [2] |
| 7 m $Zn(ClO_4)_2$-succinonitrile | 0.5 $mA/cm^2$; 0.5 $mAh/cm^2$ | 98.4% | [3] |
| 21 m LiTFSI-3 m $Zn(OTf)_2$ | 1 $mA/cm^2$; 1 $mAh/cm^2$ | 99.0% (After 15 cycles) | [4] |
| 1 m $Zn(OAc)_2$-31 m KOAc | 0.8 $mA/cm^2$; 0.8$mAh/cm^2$ | 99.2% | [5] |
| 4.2 M $ZnSO_4$ + 0.1 M $MnSO_4$ | 0.5 $mA/cm^2$; 1 $mAh/cm^2$ | 99.2% | [6] |
| 30 m $ZnCl_2$ | 0.2 $mA/cm^2$; 0.4 $mAh/cm^2$ | 95.4% | [7] |
| 1 m $Zn(OTf)_2$-acetonitrile | 0.5 $mA/cm^2$; 1 $mAh/cm^2$ | 99.3% | [8] |
| 2 M $ZnSO_4$-ethylene glycol | 0.5 $mA/cm^2$; 1 $mAh/cm^2$ | 99% | [9] |
| 1 M $ZnSO_4$-polyethylene oxide | 1 $mA/cm^2$; 1 $mAh/cm^2$ | 99.5% | [10] |

## Reference


[1] L. Cao, D. Li, E. Hu, J. Xu, T. Deng, L. Ma, Y. Wang, X. Q. Yang, C. Wang, *J Am Chem Soc*, 2020, **14**, 21404-21409.

[2] H. Qiu, X. Du, J. Zhao, Y. Wang, J. Ju, Z. Chen, Z. Hu, D. Yan, X. Zhou, G. Cui, *Nat Commun*, 2019, **10**, 1-12.

[3] W. Yang, X. Du, J. Zhao, Z. Chen, J. Li, J. Xie, Y. Zhang, Z. Cui, Q. Kong, Z. Zhao, C. Wang, Q. Zhang, G. Cui, *Joule*, 2020, 4, 1557-1574.

[4] H. Zhang, X. Liu, H. Li, B. Qin, S. Passerini, *ACS Appl Mater Interfaces*, 2020, **12**, 15305-15312.

[5] S. Chen, R. Lan, J. Humphreys, S. Tao, *Energy Storage Mater*, 2020, **28**, 205-215.

[6] B. W. Olbasa, F. W. Fenta, S.F. Chiu, M.C. Tsai, C.J. Huang, B. A. Jote, T. T. Beyene, Y.F. Liao, C.H. Wang, W.N. Su, H. Dai, B. J. Hwang, *ACS Appl. Energy Mater*, 2020, **3**, 4499-4508.

[7] C. Zhang, J. Holoubek, X. Wu, A. Daniyar, L. Zhu, C. Chen, D. P. Leonard, I. A. Rodriguez-Perez, J. X. Jiang, C. Fang, X. Ji, *Chem Commun (Camb),* 2018, **54**, 14097-14099.

[8] J. Shi, K. Xia, L. Liu, C. Liu, Q. Zhang, L. Li, X. Zhou, J. Liang, Z. Tao, *Electrochimica Acta*, 2020, **358**, 136937.

[9] N. Chang, T. Li, R. Li, S. Wang, Y. Yin, H. Zhang, X. Li, *Energy Environ. Sci*, 2020, **13**, 3527-3535.

[10] Y. Jin, K. S. Han, Y. Shao, M. L. Sushko, J. Xiao, H. Pan, J. Liu, *Adv. Funct. Mater,* 2020, **30**, 2003932.